THE COMBINATORICS OF FRIEZE PATTERNS AND MARKOFF NUMBERS

James Propp
Department of Mathematics, UMass Lowell, Lowell, Massachusetts
jamespropp.org

Received: 9/7/19, Accepted: 1/24/20, Published: 2/14/20

Abstract

This article, based on joint work with Gabriel Carroll, Neil Herriot, Andy Itsara, Ian Le, Gregg Musiker, Gregory Price, Dylan Thurston, and Rui Viana, presents a combinatorial model based on perfect matchings that explains the symmetries of the numerical arrays that Conway and Coxeter dubbed frieze patterns. This matchings model is a combinatorial interpretation of Fomin and Zelevinsky's cluster algebras of type A. One can derive from the matchings model an enumerative meaning for the Markoff numbers, and prove that the associated Laurent polynomials have positive coefficients as was conjectured (much more generally) by Fomin and Zelevinsky.

– Dedicated to the memory of Horst Sachs, 1927–2016

1. Introduction

This article is part of a recent burst of activity relating to what Sergey Fomin and Andrei Zelevinsky have dubbed the "Laurent phenomenon" [19] (described in greater detail below), This phenomenon has algebraic, topological, and combinatorial aspects, and it the third of these aspects that is developed here. In particular, we show how two examples of rational recurrences — the two-dimensional frieze patterns of Conway and Coxeter, and the tree of Markoff numbers — relate to one another and to the Laurent phenomenon.

A *Laurent polynomial* in the variables $x, y, \ldots$ is a rational function in $x, y, \ldots$ that can be expressed as a polynomial in the variables $x, x^{-1}, y, y^{-1}, \ldots$; for example, the function $f(x) = (x^2 + 1)/x = x + x^{-1}$ is a Laurent polynomial, but the composition $f(f(x)) = (x^4+3x^2+1)/x(x^2+1)$ is not. The preceding example shows that the set of Laurent polynomials in a single variable is not closed under composition. This failure of closure also holds in the multivariate setting; for instance, if $f(x, y)$, $g(x, y)$ and $h(x, y)$ are Laurent polynomials in x and y, then we would not expect to find that $f(g(x, y), h(x, y))$ is a Laurent polynomial as well. Nonetheless,

it has been discovered that, in broad class of instances (embraced as yet by no general rule), "fortuitous" cancellations occur that cause Laurentness to be preserved. This is the "Laurent phenomenon" discussed by Fomin and Zelevinsky [19].

Furthermore, in many situations where the Laurent phenomenon holds, there is a positivity phenomenon at work as well, and all the coefficients of the Laurent polynomials turn out to be positive. In these cases, the functions being composed are Laurent polynomials with positive coefficients; that is, they are expressions involving only addition, multiplication, and division. It should be noted that subtraction-free expressions do not have all the closure properties one might hope for, as the example $(x^3 + y^3)/(x + y)$ illustrates: although the expression is subtraction-free, its reduced form $x^2 - xy + y^2$ is not.

Fomin and Zelevinsky have shown that a large part of the Laurentness phenomenon fits in with their general theory of cluster algebras. This article will treat one important special case of the Laurentness-plus-positivity phenomenon, namely the case associated with cluster algebras of type A, discussed in detail in [20]. The purely combinatorial approach taken in Sections 2 and 3 of this article obscures the links with deeper issues (notably the representation-theoretic questions that motivated the invention of cluster algebras), but it provides the quickest and most self-contained way to prove the Laurentness-plus-positivity assertion in this case (Theorem 2). The frieze patterns of Conway and Coxeter [12], and their link with triangulations of polygons, will play a fundamental role, as will perfect matchings of graphs derived from these triangulations. (For a different, more algebraic way of thinking about frieze patterns, see [8]. For an extension of the result of this article into a broader setting, see [2].)

In Sections 5 and 6 of this article, two variations on the theme of frieze patterns are considered. One is the tropical analogue, which has bearing on graph-metrics in trees. The other variant is based on a recurrence that looks very similar to the frieze relation; the variant recurrence appears to give rise to tables of positive integers possessing the same glide-reflection symmetry as frieze patterns, but positivity and integrality are still unproved as of 2005.

In Section 4, the graphs constructed in Section 2 are viewed from a number of different perspectives that relate them to existing literature.

In Section 7, the constructions of Sections 2 and 3 are specialized to a case in which the triangulated polygons come from pairs of mutually visible points in a dissection of the plane into equilateral triangles. In this case, counting the matchings of the derived graphs gives us an enumerative interpretation of Markoff numbers (numbers satisfying the ternary cubic $x^2 + y^2 + z^2 = 3xyz$). This yields a combinatorial proof of a Laurentness assertion proved by Fomin and Zelevinsky in [19] (namely a special case of their Theorem 1.10) that falls outside of the framework of cluster algebras in the strict sense. Fomin and Zelevinsky proved Theorem 1.10 by use of their versatile "Caterpillar Lemma", but this proof did not settle the issue

of positivity. The combinatorial approach adopted here shows that all of the Laurent polynomials that occur in the three-variable rational-function analogue of the Markoff numbers — the "Markoff polynomials" — are in fact positive (Theorem 5).

Section 8 concludes with some problems suggested by the main result of Section 7. One can try to generalize the combinatorial picture by taking other dissections of the plane into triangles, or one can try to generalize by considering other Diophantine equations. There are tantalizing hints of a link between the two proposed avenues of generalization, but its nature is still obscure.

Most of this research was conducted with support from the National Science Foundation and the National Security Agency, with additional support from Harvard University and the Massachusetts Institute of Technology. From 2001 to 2003 the author met with roughly twenty Boston-area undergraduates as part of a program called REACH (Research Experiences in Algebraic Combinatorics at Harvard). This article would not exist without the deep insight and hard work of Gabriel Carroll, Neil Herriot, Andy Itsara, Ian Le, Andy Itsara, Ian Le, Gregg Musiker, Gregory Price, and Rui Viana (all of whom were undergraduates at the time the work was done). Also helpful were conversations with Rick Kenyon, David Speyer, Dylan Thurston, and David Wilson. The article was posted on the arXiv in 2005, but it was never formally published. The author is grateful to Jeffrey Lagarias for encouraging him to belatedly publish the article in INTEGERS. Much work has been done on frieze patterns in the intervening fifteen years; this article makes no attempt to situate the work of REACH relative to the current state of the field.

2. Triangulations and Frieze Patterns

A *frieze pattern* [12] is an infinite array such as

...	1		1		1		1		1		1		1		1		1		...
...		$\frac{5}{3}$		2		1		5		$\frac{2}{3}$		3		$\frac{5}{3}$		2		...	
...	4		$\frac{7}{3}$		1		4		$\frac{7}{3}$		1		4		$\frac{7}{3}$			...	
...		5		$\frac{2}{3}$		3		$\frac{5}{3}$		2		1		5		$\frac{2}{3}$		...	
...	1		1		1		1		1		1		1		1			...	

consisting of $n-1$ rows, each periodic with period n, such that all entries in the top and bottom rows are equal to 1 and all entries in the intervening rows satisfy the relation

$$\begin{array}{ccc} & A & \\ B & & C \\ & D & \end{array} \quad : \quad AD = BC - 1 \ .$$

The rationale for the term "frieze pattern" is that such an array automatically possesses glide-reflection symmetry (as found in some decorative friezes): for $1 \leq m \leq n-1$, the $(n-m)$th row is the same as the mth row, shifted rightward (or, equivalently, leftward) by $n/2$ positions. Hence the relation $AD = BC - 1$ will be referred to below as the "frieze relation" even though its relevance to friezes and their symmetries is not apparent from the algebraic definition.

Frieze patterns arose from Coxeter's study of metric properties of polytopes, and served as useful scaffolding for various sorts of metric data; see e.g. [14] (page 160), [15], and [16]. Typically some of the entries in a metric frieze pattern are irrational. Conway and Coxeter completely classify the frieze patterns whose entries are positive integers, and show that these frieze patterns constitute a manifestation of the Catalan numbers. Specifically, there is a natural association between positive integer frieze patterns and triangulations of regular polygons with labeled vertices. (In addition to [12], see the shorter discussion on pp. 74–76 and 96–97 of [13].) Note that for each fixed n, any convex n-gon would serve here just as well as the regular n-gon, since we are only viewing triangulations combinatorially.

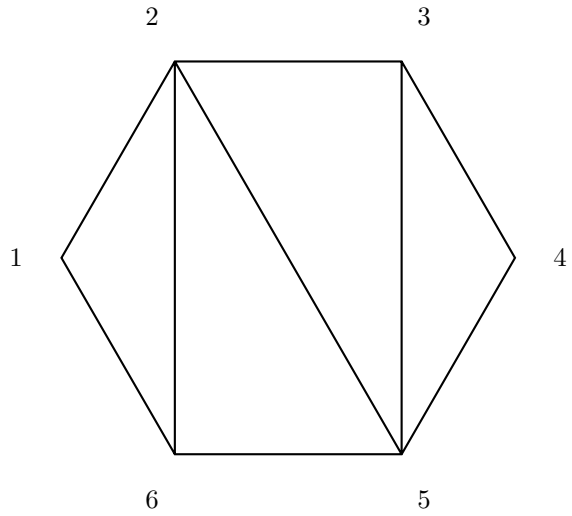

Figure 1. A triangulated 6-gon.

From every triangulation T of a regular n-gon with vertices cyclically labeled 1 through n, Conway and Coxeter build an $(n-1)$-rowed frieze pattern determined by the numbers $a_1, a_2, \ldots, a_n$, where a_k is the number of triangles in T incident with vertex k. Specifically: (1) the top row of the array is $\ldots, 1, 1, 1, \ldots$; (2) the second row (offset from the first) is $\ldots, a_1, a_2, \ldots, a_n, a_1, \ldots$ (with period n); and (3) each

succeeding row (offset from the one before) is determined by the frieze recurrence

$$\begin{array}{ccc} & A & \\ B & & C \\ & D & \end{array} \quad : \quad D = (BC-1)/A \ .$$

For example, the triangulation shown in Figure 1 determines the data $(a_1, \ldots, a_6) = (1, 3, 2, 1, 3, 2)$ and the 5-row frieze pattern

$$\begin{array}{ccccccccccccccccccc}
\ldots & 1 & & 1 & & 1 & & 1 & & 1 & & 1 & & 1 & \ldots \\
\ldots & & 1 & & 3 & & 2 & & 1 & & 3 & & 2 & & \ldots \\
\ldots & 1 & & 2 & & 5 & & 1 & & 2 & & 5 & & 1 & \ldots \\
\ldots & & 1 & & 3 & & 2 & & 1 & & 3 & & 2 & & \ldots \\
\ldots & 1 & & 1 & & 1 & & 1 & & 1 & & 1 & & 1 & \ldots
\end{array}$$

Conway and Coxeter show that the frieze relation, applied to the initial rows $\ldots, 1, 1, 1, \ldots$ and $\ldots, a_1, a_2, \ldots, a_n, \ldots$, yields a frieze pattern. Note that implicit in this assertion is the proposition that every entry in rows 1 through $n-3$ is non-zero (so that the recurrence $D = (BC-1)/A$ never involves division by 0). It is not a priori obvious that each of the entries in the array is positive (since the recurrence involves subtraction) or that each of the entries is an integer (since the recurrence involves division). Nor is it immediately clear why for $1 \leq m \leq n-1$, the $(n-m)$th row of the table given by repeated application of the recurrence should be the same as the mth row, shifted, so that in particular the $(n-1)$st row, like the first row, consists entirely of 1's.

These and many other properties of frieze patterns are explained by a combinatorial model of frieze patterns discovered by Carroll and Price [10] (based on earlier work of Itsara, Le, Musiker, Price, and Viana; see [27] and [33], as well as [9]). Given a triangulation T as above, define a bipartite graph $G = G(T)$ whose n black vertices v correspond to the vertices of T, whose $n-2$ white vertices w correspond to the triangular faces of T, and whose edges correspond to all incidences between vertices and faces in T (that is, v and w are joined by an edge precisely if v is one of the three vertices of the triangle in T associated with w). For $i \neq j$ in the range $1, ..., n$, let $G_{i,j}$ be the graph obtained from G by removing black vertices i and j and all edges incident with them, and let $m_{i,j}$ be the number of perfect matchings of $G_{i,j}$ (that is, the number of ways to pair all $n-2$ of the black vertices with the $n-2$ white vertices, so that every vertex is paired to a vertex of the opposite color adjacent to it). For instance, for the triangulation T of the 6-gon defined in Figure 1, the graph $G_{1,4}$ is as shown in Figure 2, and we have $m_{1,4} = 5$ since this graph has 5 perfect matchings.

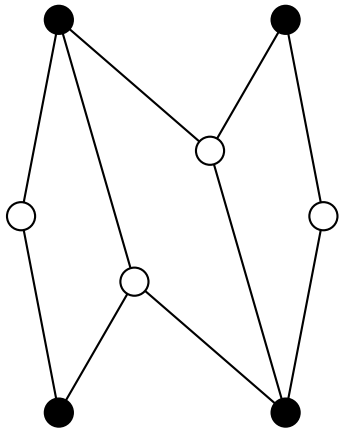

Figure 2. The graph $G_{1,4}$.

Theorem 1 (Carroll and Price [10])**.** *The Conway-Coxeter frieze pattern of a triangulation T is just the array*

$$\begin{array}{ccccccccccc}
\ldots & & m_{1,2} & & m_{2,3} & & m_{3,4} & & m_{4,5} & & \ldots \\
\ldots & & & m_{1,3} & & m_{2,4} & & m_{3,5} & & & \ldots \\
\ldots & & m_{n,3} & & m_{1,4} & & m_{2,5} & & m_{3,6} & & \ldots \\
\ldots & & & m_{n,4} & & m_{1,5} & & m_{2,6} & & & \ldots \\
& & \vdots & & \vdots & & \vdots & & \vdots & &
\end{array}$$

where here as hereafter we interpret all subscripts mod n.

Note that this claim makes the glide-reflection symmetry of frieze patterns a trivial consequence of the fact that $G_{i,j} = G_{j,i}$.

Proof. Here is a sketch of the main steps of the proof:

(1) $m_{i,i+1} = 1$: This holds because there is a tree structure on the set of triangles in T that induces a tree structure on the set of white vertices of G. If we examine the white vertices of G, proceeding from outermost to innermost, we find that we have no freedom in how to match them with black vertices, when we keep in mind that every black vertex must be matched with a white vertex. (In fact, the same reasoning shows that $m_{i,j} = 1$ whenever the triangulation T contains a diagonal connecting vertices i and j.)

(2) $m_{i-1,i+1} = a_i$: The argument is similar, except now we have some freedom in how the ith black vertex is matched: it can be matched with any of the a_i adjacent white vertices.

(3) $m_{i,j}\, m_{i-1,j+1} = m_{i-1,j}\, m_{i,j+1} - 1$: If we move the 1 to the left-hand side, we can use (1) to write the equation in the form

$$m_{i,j}\, m_{i-1,j+1} + m_{i-1,i}\, m_{j,j+1} = m_{i-1,j}\, m_{i,j+1}.$$

This relation is a direct consequence of a lemma due to Eric Kuo (Theorem 2.5 in [30]), which is stated here for the reader's convenience:

Condensation lemma: If a bipartite planar graph G has 2 more black vertices than white vertices, and the black vertices a, b, c, d lie in cyclic order on some face of G, then

$$m(a,c)m(b,d) = m(a,b)m(c,d) + m(a,d)m(b,c),$$

where $m(x,y)$ denotes the number of perfect matchings of the graph obtained from G by deleting vertices x and y and all incident edges.

(1) and (2) tell us that Carroll and Price's theorem applies to the first two rows of the frieze pattern, and (3) tells us (by induction) that the theorem applies to all subsequent rows. □

It should be mentioned that Conway and Coxeter give an alternative way of describing the entries in frieze patterns, as determinants of tridiagonal matrices. Note that $m_{i-1,i+1} = a_i$ which equals the determinant of the 1-by-1 matrix whose sole entry is a_i, while $m_{i-1,i+2} = a_i a_{i+1} - 1$ which equals the determinant of the 2-by-2 matrix

$$\begin{pmatrix} a_i & 1 \\ 1 & a_{i+1} \end{pmatrix}.$$

One can show by induction using Dodgson's determinant identity (for a statement and a pretty proof of this identity see [41]) that $m_{i-1,i+k}$ equals the Euler continuant $[a_i, \ldots, a_{i+k-1}]$, that is, the determinant of the k-by-k matrix with entries $a_i, \ldots, a_{i+k-1}$ down the diagonal, 1's in the two flanking diagonals, and 0's everywhere else. This is true for any array satisfying the frieze relation whose initial row consists of 1's, whether or not it is a frieze pattern. Thus, any numerical array constructed via the frieze relation from initial data consisting of a first row of 1's and a second row of integers will be an array of integers, since entries in subsequent rows are equal to determinants of integer matrices. (One caveat is in order here: although the table of tridiagonal determinants always satisfies the frieze relation, it may not be possible to compute the table using just the frieze relation, since some of the expressions that arise might be indeterminate fractions of the form 0/0.) However, for most choices of positive integers $a_1, \ldots, a_n$, the resulting table of integers will not be an $(n-1)$-rowed frieze pattern, because some entries lower down in the table will be negative (or vanish). Indeed, Conway and Coxeter show

that every $(n-1)$-rowed frieze pattern whose entries are positive integers arises from a triangulated n-gon in the fashion described above.

3. The Sideways Recurrence and Its Periodicity

Recall that any $(n-1)$-rowed array of real numbers that begins and ends with rows of 1's and satisfies the frieze relation in between, with all rows having period n, qualifies as a frieze pattern.

Note that if the vertices $1, \ldots, n$ of an n-gon lie on a circle and we let $d_{i,j}$ be the distance between points i and j, Ptolemy's theorem on the lengths of the sides and diagonals of an inscriptible quadrilateral gives us the three-term quadratic relation

$$d_{i,j}\, d_{i-1,j+1} + d_{i-1,i}\, d_{j-1,j} = d_{i-1,j}\, d_{i,j+1}$$

(with all subscripts interpreted mod n). Hence the numbers $d_{i,j}$ with $i \neq j$, arranged just as the numbers $m_{i,j}$ were, form an $(n-1)$-rowed array that almost qualifies as a frieze pattern (the array satisfies the frieze relation and has glide-reflection symmetry because $d_{i,j} = d_{j,i}$ for all i, j, but the top and bottom rows do not in general consist of 1's). The nicest case occurs when the n-gon is a regular n-gon of side-length 1; then we get a genuine frieze pattern and each row of the frieze pattern is constant.

Another source of frieze patterns is an old result from spherical geometry: the *pentagramma mirificum* of Napier and Gauss embodies the assertion that the arc-lengths of the sides in a right-angled spherical pentagram can be arranged to form the middle two rows of a four-rowed frieze pattern.

Conway and Coxeter show that frieze patterns are easy to construct if one proceeds not from top to bottom (since one is unlikely to choose numbers $a_1, \ldots, a_n$ in the second row that will yield all 1's in the $(n-1)$st row) but from left to right, starting with a zig-zag of entries connecting the top and bottom rows (where the zig-zag path need not alternate between leftward steps and rightward steps but may consist of any pattern of leftward steps and rightward steps), using the sideways frieze recurrence

$$\begin{array}{ccc} & A & \\ B & & C \\ & D & \end{array} \quad : \quad C = (AD+1)/B$$

Although a priori one might imagine that repeating this recurrence would lead one to non-integer rational numbers whose numerators and denominators would get increasingly large as one goes from left to right, it turns out that the resulting pattern necessarily repeats with period n, and that all the numbers that appear are whole numbers (provided that all the entries in the initial zig-zag are equal to 1).

For example, consider the partial frieze pattern

$$\begin{array}{ccccccccccc} \ldots & 1 & & 1 & & 1 & & 1 & & 1 & \ldots \\ & & x & & x' & & & & & & \\ & y & & y' & & & & & & & \\ & & z & & z' & & & & & & \\ \ldots & 1 & & 1 & & 1 & & 1 & & 1 & \ldots \end{array}$$

Given non-zero values of x, y, and z, one can successively compute $y' = (xz+1)/y$, $x' = (y'+1)/x$, and $z' = (y'+1)/z$, obtaining a new zig-zag of entries x', y', z' connecting the top and bottom rows. It is clear that for generic choices of non-zero x, y, z, one has x', y', z' non-zero as well, so the procedure can be repeated, yielding further zig-zags of entries. After six iterations of the procedure one recovers the original numbers x, y, z six places to the right of their original position (unless one has unluckily chosen x, y, z so as to cause one to encounter an indeterminate expression of the form $0/0$ from the recurrence), and if we specialize to $x = y = z = 1$, we get the 5-row frieze pattern associated with Figure 1.

To dodge the issue of indeterminate expressions of the form $0/0$, we embrace indeterminacy of another sort by regarding x, y, z as formal quantities, not specific numbers, so that x', y', z', etc. become rational functions of x, y, and z. Then our recurrence ceases to be problematic. Indeed, one finds that the rational functions that arise are of a special kind, namely, Laurent polynomials with positive coefficients.

We can see why this is so by incorporating weighted edges into our matchings model. Returning to the triangulated hexagon from Section 2, associate the values x, y, and z with the diagonals joining vertices 2 and 6, vertices 2 and 5, and vertices 3 and 5, respectively. Call these the formal weights of the diagonals. Also assign weight 1 to each of the 6 sides of the hexagon; see Figure 3.

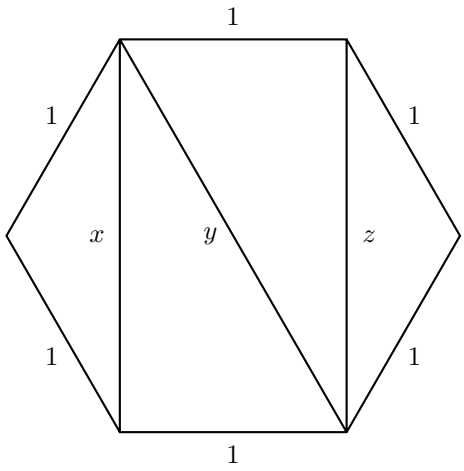

Figure 3. A triangulated 6-gon with edge-weights.

Now construct the graph G from the triangulation as before, this time assigning weights to all the edges. Specifically, if v is a black vertex of G that corresponds to a vertex of the n-gon and w is a white vertex of G that corresponds to a triangle in the triangulation T that has v as one of its three vertices (and has v' and v'' as the other two vertices), then the edge in G that joins v and w should be assigned the weight of the side or diagonal in T that joins v' and v''; see Figure 4.

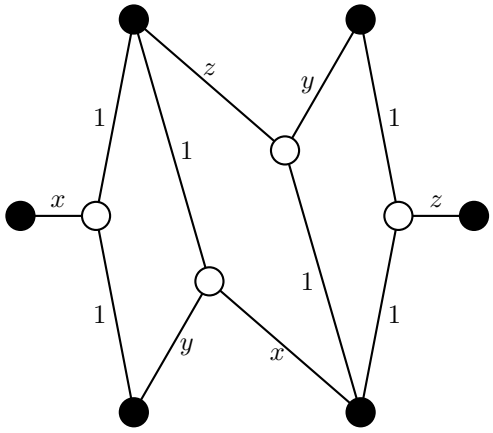

Figure 4. The graph $G_{1,4}$ with edge-weights.

We now define $W_{i,j}$ as the sum of the weights of all the perfect matchings of the graph $G_{i,j}$ obtained from G by deleting vertices i and j (and all their incident

edges), where the weight of a perfect matching is the product of the weights of its constituent edges, and we define $M_{i,j}$ as $W_{i,j}$ divided by the product of the weights of all the diagonals (this product is xyz in our running example); e.g., $W_{1,4} = 1+2y+y^2+xz$ and $M_{1,4} = x^{-1}y^{-1}z^{-1}+2x^{-1}z^{-1}+x^{-1}yz^{-1}+y^{-1}$. These $M_{i,j}$'s, which are rational functions of x, y, and z, generalize the numbers denoted by $m_{i,j}$ earlier, since we recover the $m_{i,j}$'s from the $M_{i,j}$'s by setting $x = y = z = 1$. It is clear that each $W_{i,j}$ is a polynomial with positive coefficients, so each $M_{i,j}$ is a Laurent polynomial with positive coefficients. And, because of the normalization (division by xyz), we have gotten each $M_{i,i+1}$ to equal 1. So the table of rational functions $M_{i,j}$ is exactly what we get by running our recurrence from left to right. When we pass from x, y, z to x', y', z', we are effectively rotating our triangulation by one-sixth of a full turn; six iterations bring us back to where we started.

It is not hard to see that the same approach works for any triangulation of an n-gon for any n, and in this way we can prove:

Theorem 2. *Given any assignment of formal weights to $n-3$ entries in an $(n-1)$-rowed table that form a zig-zag joining the top row (consisting of all 1's) to the bottom row (consisting of all 1's), there is a unique assignment of rational functions to all the entries in the table so that the frieze relation is satisfied. These rational functions of the original $n-3$ variables have glide-reflection symmetry that gives each row period n. Furthermore, each of the rational functions in the table is a Laurent polynomial with positive coefficients.*

Note that a zig-zag joining the top row to the bottom row corresponds to a triangulation T whose dual tree is just a path. Not every triangulation is of this kind (for instance, consider the hexagon shown in Figure 1 triangulated by diagonals joining vertices 2 and 4, vertices 4 and 6, and vertices 2 and 6). In general, the entries in a frieze pattern that correspond to the diagonals of a triangulation T do not form a zig-zag path, so it is not clear from the frieze pattern how to extend the known entries to the unknown entries (e.g., for the triangulation described in the parenthetical remark in the previous sentence, if one assigns respective weights x, y, and z to the specified diagonals, one obtains the partial frieze pattern

$$\begin{array}{ccccccccccccccc}
\ldots & 1 & & 1 & & 1 & & 1 & & 1 & & 1 & & \ldots \\
\ldots & & ? & & x & & ? & & y & & ? & & z & \ldots \\
\ldots & ? & & ? & & ? & & ? & & ? & & ? & & \ldots \\
\ldots & & y & & ? & & z & & ? & & x & & ? & \ldots \\
\ldots & 1 & & 1 & & 1 & & 1 & & 1 & & 1 & & \ldots
\end{array}$$

where the question marks refer to entries whose values do not follow immediately from the frieze recurrence). In such a case, it is best to refer directly to the triangulation itself, and to use a generalization of the frieze relation, namely the (formal)

Ptolemy relation [10]

$$M_{i,j}\,M_{k,l} + M_{j,k}\,M_{i,l} = M_{i,k}\,M_{j,l}$$

where i, j, k, l are four vertices of the n-gon listed in cyclic order. (Conway and Coxeter [12] give spatially extended versions of the frieze relation that are equivalent to special cases of the Ptolemy relation.) Since every triangulation of a convex n-gon can be obtained from every other by means of flips that replace one diagonal of a quadrilateral by the other diagonal (an observation that goes back at least as far as 1936 [39]), we can iterate the Ptolemy relation so as to solve for all of the $M_{i,j}$'s in terms of the ones whose values were given.

Up until now we have associated indeterminates with the $n-3$ diagonals, but not the n sides, of our triangulated n-gon. If we assign formal indeterminates to the sides as well as the diagonals and carry out the construction of the edge-weighted graph $G_{i,j}$ (incorporating the n new variables) and the polynomial $W_{i,j}$ (the sum of the weights of all the perfect matchings of $G_{i,j}$), and we define the Laurent polynomial $M_{i,j}$ as $W_{i,j}$ divided by the product of all $n-3$ diagonal-weights, the proof of Theorem 2 still goes through, and one sees that the $M_{i,j}$'s form an array in which the top and bottom rows contain the indeterminates associated with the sides of the n-gon and the intervening rows satisfy the modified frieze relation

$$\begin{array}{ccccc} X & & & & Y \\ & \ddots & A & \iddots & \\ & B & & C & \\ & \iddots & D & \ddots & \\ Y & & & & X \end{array} \qquad : \qquad BC = AD + XY$$

where X is the top entry in the diagonal containing B and D as well as the bottom entry in the diagonal containing A and C and Y is the top entry in the diagonal containing C and D as well as the bottom entry in the diagonal containing A and B. Each entry in this generalized frieze pattern is a Laurent monomial in the $2n-3$ variables in which the n variables associated with sides of the n-gon occur in only with non-negative exponents.

Our combinatorial construction of Laurent polynomials associated with the sides and diagonals of an n-gon is essentially nothing more than the type A case (more precisely, the A_{n-3} case) of the cluster algebra construction of Fomin and Zelevinsky [20]. The result that our matchings model yields, stated in a self-contained way, is as follows:

Theorem 3. *Given any assignment of formal weights $x_{i,j}$ to the $2n-3$ edges of a triangulated convex n-gon, (where $x_{i,j}$ is associated with the edge joining vertices i and j), there is a unique assignment of rational functions to all $n(n-3)/2$*

diagonals of the n-gon such that the rational functions assigned to the four sides and two diagonals of any quadrilateral determined by four of the n vertices satisfy the Ptolemy relation. These rational functions of the original $2n-3$ variables are Laurent polynomials with positive coefficients.

The formal weights are precisely the cluster variables in the cluster algebra of type A_{n-3}, and the triangulations are the clusters. The periodicity phenomenon is a special case of a more general periodicity conjectured by Zamolodchikov and proved in the type A case independently by Frenkel and Szenes and by Gliozzi and Tateo; see [20] for details.

4. Snake Graphs

The bipartite graphs $G_{i,j}$ obtained in Section 2, when shorn of their forced edges (edges that belong to every perfect matching) and their forbidden edges (edges that belong to no perfect matching), have a direct combinatorial construction as "snakes" of 4-cycles, obtained by repeating the process of adding a new 4-cycle at the end of a snake. More precisely: a snake of order 0 is just two vertices joined by an edge; a snake of order 1 is a 4-cycle; a snake of order 2 is a pair of 4-cycles sharing a single edge, obtained by adjoining one 4-cycle to another along an edge; and if one has a snake of order $k-1$ whose most recently added 4-cycle C was adjoined along edge e, one obtains a snake of order k by adjoining a new 4-cycle that shares some edge of C other than e. For example, Figure 5 shows a snake of order 6 obtained from a triangulated 9-gon whose vertices are shown in black (the two vertices represented by smaller black dots are not part of the snake, but they are included for clarity). Given a triangulation T, the only edges of $G_{i,j}$ that are neither forced nor forbidden are those whose white endpoint corresponds to a triangle in T on the path of triangles joining vertices i and j. These edges form a snake-graph whose twists and turns mimic those of the path of triangles.

Up until now, we have used n to denote the number of sides of the polygon being triangulated, but in this section it will be more convenient to let $n+3$ denote the number of sides of the polygon, and to make the additional assumption that every triangle in the triangulation of the $(n+3)$-gon occurs on the path of triangles from i to j, so that the graph $G_{i,j}$ has no forced or forbidden edges and the snake-graph has order n.

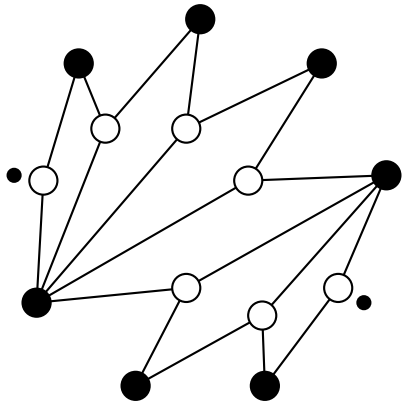

Figure 5. A snake of order 6.

Although the operation of adding on a new 4-cycle, or "box", can be done in three ways at each step in the iterative construction of a snake, for purposes of counting perfect matchings there are really only two choices at each stage: for $k \geq 3$, the edge that joins the $(k-1)$st box to the kth can either (1) be disjoint from the edge that joins the $(k-2)$nd box to the $(k-1)$st or (2) have an endpoint in common with it. If we let m_k, m_{k-1}, and m_{k-2} denote the number of perfect matchings of the kth, $(k-1)$st, and $(k-2)$nd snakes in the iterative process, then (as we will now show) in case 1, $m_k = m_{k-1} + m_{k-2}$, while in case 2, $m_k = m_{k-1} + (m_{k-1} - m_{k-2})$; that is, the three numbers are either in "Fibonacci progression" or in arithmetic progression. Refer to Figure 6, where u and v are the vertices of the $(k-2)$nd snake that are not part of the $(k-3)$rd snake, w and x are the vertices of the $(k-1)$st snake that are not part of the $(k-2)$nd snake, and y and z are the vertices of the kth snake that are not part of the $(k-1)$st snake, in the fashion shown. In both cases, the difference $m_k - m_{k-1}$ counts those perfect matchings of the kth snake that do not contain the edge yz and that are therefore forced to contain all the edges shown in bold in the figure. In case 1, these perfect matchings correspond to perfect matchings of the $(k-2)$nd snake: simply delete edges wy and xz (and the vertices they contain). In case 2, these perfect matchings correspond to those perfect matchings of the $(k-1)$st snake that do not arise from a perfect matching of the $(k-2)$nd snake by adjoining the edge wx: simply delete edges vy and xz

and adjoin edge vx.

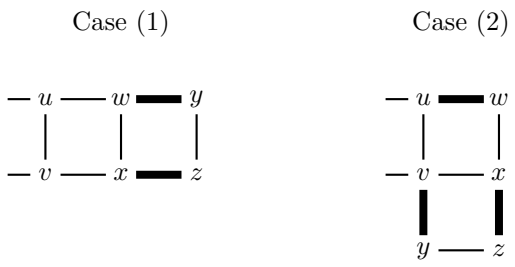

Figure 6. The snake-graph recurrence.

In terms of the triangulation picture, a snake-graph of order k corresponds to a chain of $k+1$ triangles, in which the ith triangle (for $2 \leq i \leq k+1$) consists of one edge uv of the $(i-1)$st triangle (not the edge joining the $(i-1)$st and $(i-2)$nd triangles) together with a new vertex x and two edges ux, vx. Any two consecutive triangles in this chain share two vertices, and any three consecutive triangles in this chain share one vertex. If the last four consecutive triangles in the chain have no vertex in common, then we are in case 1; if they do have a vertex in common, we are in case 2. We can make a *code* of length $n-2$ that contains this information. Thus, the snake-graph shown in Figure 5 and the triangulation it arises from can be described (from left to right) by the code **2212**, indicating that as we move through the snake from left to right, we encounter case 2, case 2, case 1, and case 2. Two extreme cases are the snake with code **11**...**1** (the "straight snake") and the snake with code **22**...**2** (the "fan snake").

For purposes of enumeration of matchings, every snake graph can be built as a chain of boxes where each new box is either added at the right of the preceding box or at the bottom of the preceding box. This is because the two geometrically distinct subcases of case 2 are the same from the point of view of enumeration of matchings, even though they are not isomorphic as graphs. For instance, consider a triangulated $(n+3)$-gon in which all the diagonals emanate from a single vertex. Strictly speaking, the associated snake (with code **22**...**2**) has all n of its boxes sharing a single vertex. However, we can replace this by a snake of squares in the square grid, where new squares are alternately added at the right or at the bottom of the growing snake. Both snake-graphs have exactly $n+1$ perfect matchings. Similarly, the snake-graph shown in Figure 5 and the snake-graph shown in Figure 7 both have the code **2212** and both have 13 perfect matchings.

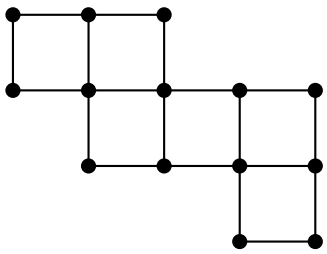

Figure 7. Another snake of order 6.

Graphs made of chains of hexagons have been considered before, starting in the chemical literature on account of their relevance to the study of benzenoid hydrocarbons; an analogous theory applies there. To add the kth hexagon to the chain, we choose one of the three edges of the $(k-1)$st hexagon that has no endpoints in common with the edge that joins the $(k-1)$st and $(k-2)$nd hexagons in the chain. If these two edges are diametrically opposite one another in the hexagon that they both belong to, we are in case 2, and the relation $m_k - m_{k-1} = m_{k-1} - m_{k-2}$ applies; otherwise, we are in case 1, and the relation $m_k - m_{k-1} = m_{k-2}$ applies.

A good way to understand what is going on here comes from consideration of products of the matrices $A = \begin{pmatrix} 0 & 1 \\ 1 & 1 \end{pmatrix}$ and $B = \begin{pmatrix} 1 & 1 \\ 1 & 0 \end{pmatrix}$. A product of $n-1$ such matrices corresponds to a snake with n boxes, where the presence of an A (resp. B) as the ith factor in the matrix product (with $1 \leq i \leq n-1$) corresponds to a horizontal (resp. vertical) segment of the snake, with the $(i+1)$st box in the snake lying to the right of (resp. below) the ith box in the snake. For instance, the matrix product $ABAAB = \begin{pmatrix} 2 & 1 \\ 7 & 3 \end{pmatrix}$ corresponds to the snake-graph shown in Figure 7, with code **2212**. More generally, a product of $n-1$ matrices, each of which is either A or B, corresponds to a snake of order n whose code can be read off from the product by the following rule: If the ith and $(i+1)$st matrices in the product are the same, the ith element of the code is 1; otherwise, the ith element of the code is 2.

The number of perfect matchings of a snake is equal to the sum of the entries of the associated matrix (so that in the specific example shown, the number of perfect matchings is $2+1+7+3$). More specifically: the matrix entry in the upper left counts the perfect matchings in which both the upper-left vertex of the snake and the lower-right vertex of the snake are matched horizontally; the matrix entry in the upper right counts the perfect matchings in which the upper-left vertex is matched horizontally and the lower-right vertex is matched vertically; the matrix entry in the lower left counts the perfect matchings in which the upper-left vertex is matched vertically and the lower-right vertex is matched horizontally; and the matrix entry in the lower right counts the perfect matchings in which both the upper-left vertex

and the lower-right vertex are matched vertically. This interpretation of the entries of the product matrix is easily verified by induction.

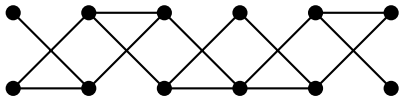

Figure 8. A paths model for snakes.

A different combinatorial model that gives the same numbers as the perfect matchings model arises from the fact that these numbers can be expressed as the sum of the entries in a matrix that is written as the product of matrices whose entries are all 0's and 1's (namely the matrices A and B). More specifically, we can create a graph in which the number of paths from either of two source vertices to either of two target vertices is the same as the number of perfect matchings of a snake-graph. Figure 8 shows what the paths-graph looks like for the snake associated with the matrix-product $ABAAB$. Each factor of A corresponds to a 4-vertex bipartite graph containing all edges from the left to the right except the edge connecting the top left to the top right, and each factor of B corresponds to a 4-vertex bipartite graph containing all edges from the left to the right except the edge connecting the bottom left to the bottom right. Multiplication of matrices corresponds to adjunction of graphs, and the definition of matrix multiplication ensures that i, jth entry of the product equals the number of left-right paths joining the jth of the two leftmost vertices to the ith of the two rightmost vertices ($1 \leq i, j \leq 2$). (For more on this combinatorial aspect of matrix multiplication, see [40].) Note that changing all A's into B's and vice versa simply flips the picture upside down.

We can improve on this model by making a slight twist in our matrix-product, working instead with the matrices $L = \begin{pmatrix} 1 & 1 \\ 0 & 1 \end{pmatrix}$ and $R = \begin{pmatrix} 1 & 0 \\ 1 & 1 \end{pmatrix}$. To turn an AB-product into an essentially equivalent LR-product, work from left to right, with the proviso that two factors in the LR product should be equal if and only if two factors in the AB product are *not*. Thus, the product $ABAAB$ corresponds to either the product $LLLRR$ or the product $RRRLL$. Either way, we get a product-matrix whose four entries are, up to permutation, the same as the four entries of the AB product, with the virtue that the picture no longer involves crossings. Figure 9, for instance, is the picture for $RRRLL$.

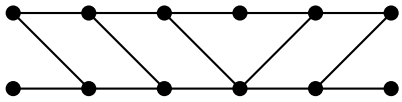

Figure 9. A planar paths model for snakes.

A variant of this picture is shown in Figure 10. This is just like the Figure 9, except that we have added a vertex at the upper left that connects to the two previously leftmost vertices, and we have added a vertex at the lower right that connects to the two previously rightmost vertices, so that, where before we counted paths from either of the two leftmost vertices to either of the two rightmost vertices (obtaining four numbers that get added together), we now count paths from the unique leftmost vertex to the unique rightmost vertex. We have marked each vertex v by a number that indicates the number of paths from the leftmost vertex to v. The leftmost vertex gets marked with a 1, and every other vertex gets marked with the sum of the numbers marking its (one or two) leftward neighbors. In terms of the triangulation, this means that we put 1's at the vertices of the initial triangle in the snake, and we proceed marking vertices along the snake all the way to its tail, where each new vertex is marked with the sum of the markings of the other two vertices of the triangle being added to the snake.

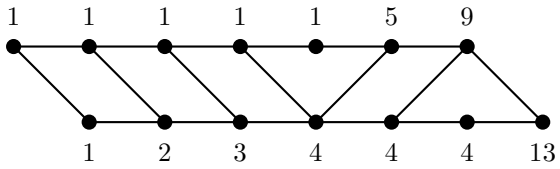

Figure 10. Another planar paths model for snakes.

The marking scheme of Figure 10 is in fact nothing more than a slight variation on Conway and Coxeter's method of computing entries in frieze patterns by successively marking the vertices in a triangulation. Conway and Coxeter mark a single vertex with a 0, all its neighbors with 1's, and proceed from there; since we are pruning away all the side-branches of the graph $G_{i,j}$ until all that remains is a snake, we are effectively limiting ourselves to the case where the vertex to be marked with a 0 has only two neighbors. In this case, the only difference between our marking scheme and Conway and Coxeter's is that they mark the initial vertex with a 0 where we mark it with a 1. Figure 11 shows what Conway and Coxeter's scheme looks like for the snake whose different representations are shown in Figures 5 through 10. The 9-gon being triangulated is not convex, but that is not a problem since we are dealing with triangulations purely combinatorially.

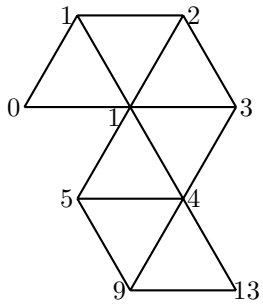

Figure 11. Conway and Coxeter's marking scheme.

At this point it should be mentioned that there is a link between the directed path model of Figure 10, the hexagon snake model, and the square snake model, by way of a multigraph matching model that is in turn related to the strip-tiling model of Benjamin and Quinn [3].

We start by making use of a correspondence that has been rediscovered a number of times [23] [35] [31], starting as far back as 1952: Let D be a directed acyclic graph with vertex set V, where m vertices $s_1, \ldots, s_m$ have been designated as sources and m other vertices $t_1, \ldots, t_m$ have been designated as targets. (Since D is acyclic, self-loops are forbidden, but D is permitted to have multiple edges.) Create an undirected graph G with vertex set $V \times \{1, 2\}$ and two kinds of edges: for each vertex v of D, D' contains an edge joining $(v, 1)$ and $(v, 2)$, and for each directed edge $e : v \to w$ of D, D' contains an edge joining $(v, 2)$ and $(w, 1)$. (If D has more than one directed edge from v to w, G has just as many edges joining $(v, 2)$ and $(w, 1)$.) Let H be the induced subgraph of G obtained by deleting all the vertices $(s_i, 1)$ and $(t_i, 2)$ $(1 \leq i \leq m)$ and all incident edges. Then the perfect matchings of H are equinumerous with the ways to join the m sources to the m targets by m edge-disjoint paths in D (which need not connect s_1 to t_1, etc.). Specifically, given such a collection of m paths, take each arc $e : v \to w$ that belongs to one of the paths and replace it by the corresponding edge joining $(v, 2)$ and $(w, 1)$ in H, and replace each vertex v in D that does not lie on any of the paths by the edge joining $(v, 1)$ and $(v, 2)$ in H. It is easy to check that this yields a perfect matching of H, and it is also easy to show that every perfect matching arises in a unique fashion in this way.

If we carry out this operation with the directed graph D shown in Figure 10 (where all edges are oriented from left to right with the leftmost vertex the sole source and the rightmost vertex the sole target), we obtain a graph G composed of

6-cycles (hexagons), as shown in Figure 12.

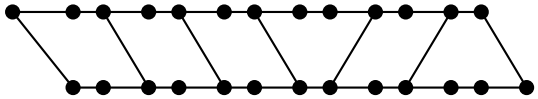

Figure 12. A hexagon snake.

Figure 13 shows how a particular path in D corresponds to a particular perfect matching in G (as described by the above proof).

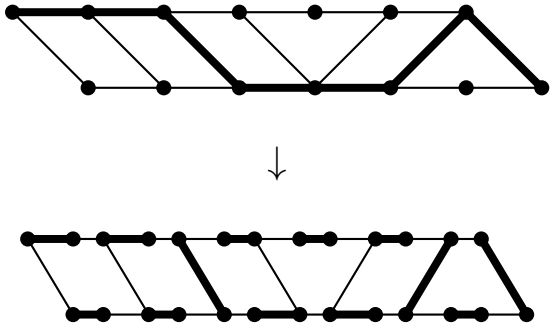

Figure 13. From path systems to perfect matchings.

The hexagon snake of Figure 12 can be drawn as a snake of regular hexagons, as shown in Figure 14. If we turn the figure on its side, so that the leftmost square is at the top, we can see how the turns of the snake correspond to the symbols in its L, R-string $RRRLL$.

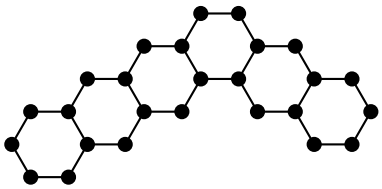

Figure 14. A hexagon snake with regular hexagons.

We also make use of an even simpler proposition that is part of the folklore of perfect matchings: Suppose v is a vertex of degree 2 in a graph G, with neighbors w_1 and w_2. Let G' be the graph obtained from G by deleting v and its two edges and identifying vertices w_1 and w_2, so that the new amalgamated vertex (call it

w) inherits the neighbors of w_1 and w_2. (Specifically, if x is some vertex that in G is connected to w_1 by m_1 edges and connected to w_2 by m_2 edges, then in G', x is connected to w by $m_1 + m_2$ edges.) Then the perfect matchings of G are equinumerous with the perfect matchings of G'. Specifically, given a perfect matching of G in which v is connected to one of w_1, w_2 and the other is connected a vertex x, construct a perfect matching of G' in which w is connected to x and all other edges are unaffected (in the case where there are multiple edges from w to x, one uses the edge that is associated with the specific edge of the matching of G that contains x).

Using this path-contraction operation, one can show that enumeration of perfect matchings of an arbitrary snake formed from n cycles of even order (i.e., any combination of 4-cycles, 6-cycles, etc., arranged in a chain consisting of n cycles) reduces to enumeration of perfect matchings of an ordinary straight snakes (made of 4-cycles) in which the edges shared by one 4-cycle and the next are allowed to have multiplicity, with multiplicities adding up to $n + 1$. These multiplicities can be easily read off from the L, R-string associated with the snake: simply duplicate the first and last symbols of the string, and then write down the run-lengths. For instance, the L, R-string $RRRLL$ becomes $RRRRLLL$ when the first and last symbols are duplicated, which gives the sequence of run-lengths $4, 3$, so that the graphs shown in Figures 7 and 13, when contracted, both become the multigraph shown in Figure 15, where the 4 represents 4 parallel edges and the 3 represents 3 parallel edges.

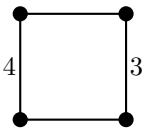

Figure 15. A (short) straight snake with multiplicities.

The perfect matchings of such a weighted graph can in turn be associated with strip-tilings of the sort considered by Benjamin and Quinn [3]. Specifically, suppose we have a straight snake of order n whose $n + 1$ vertical edges have multiplicities $r_0, r_1, \ldots, r_N$. Then we associate this with a 1-by-$(n + 1)$ rectangular strip that is to be covered by stackable 1-by-1 square tiles and non-stackable 1-by-2 rectangular tiles ("dominos"), where each square in the strip must be covered by at least one tile, and where square tiles may be stacked to height r_i at the ith square of the strip. For example, for the graph shown in Figure 15, the associated strip-tiling problem would involve a strip consisting of two squares, which can either be tiled by a single domino or by two non-empty stacks of squares (up to 4 squares in the left stack and up to 3 squares in the right stack).

By this point in the article, many readers will have recognized that our combinatorial model is not too far removed from the theory of continued fractions. Work of Benjamin and Quinn, in the context of the strip-tiling model, shows how combinatorial models can illuminate facts about continued fractions (especially those like [4] and [5] that involve reversing the order of the convergents: this operation seems unnatural from the point of view of the definition of continued fractions, inasmuch as it switches the high-order and low-order parts of the continued fraction representation, but the operation is extremely natural for tilings of a strip).

There is a different way to relate frieze patterns to snake-graphs, where we count paths in the snake-graphs themselves. For instance, the number 13, whose various enumerative interpretations we have followed throughout this section, also occurs as the number of paths from the leftmost vertex to the rightmost vertex in the hexagon snake shown in Figure 14. To see why, note that for purposes of enumerating such paths, we can shrink each horizontal edge in Figure 14 to a point (identifying the two endpoints), obtaining a square snake (see Figure 16) that is combinatorially the same as the square snake shown in Figure 10. It should be stressed that this square snake is not the square snake we started with (shown in Figure 7). It is "dual" to the original square snake, making a bend where the original snake goes straight and going straight where the original snake makes a bend. (Equivalently, the code of the first snake has a **1** where the code of the second snake has a **2**, and vice versa.) Enumerating perfect matchings of each snake is equivalent to counting paths its dual (from head to tail). For instance, the snake in Figure 7 has 13 perfect matchings and 19 paths from head to tail, while the snake in Figure 16 has 19 perfect matchings and 13 paths from head to tail.

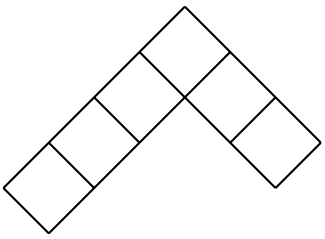

Figure 16. A dual snake.

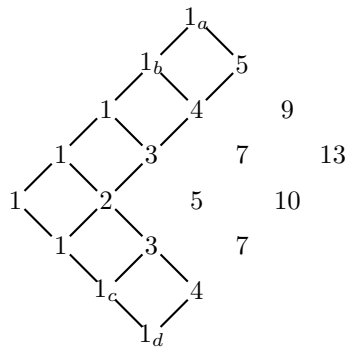

Figure 17. A dual snake in a frieze pattern.

There is a nice way to see a dual square snake of order n as residing within a frieze pattern of order $n+3$: rotate the snake by 90 degrees, so that its first cell is at the top and its last cell is at the bottom, and put its top vertex (call it u) in the initial row of 1's of an initially blank frieze pattern with $n+2$ rows, so that its bottom vertex (call it v) lands in the final row of 1's, and the R's and L's indicate whether each successive box in the snake lies to the right or left (respectively) of the previous box. If we put 1's along the left border of the snake, we get a zig-zag of the kind discussed earlier, so we obtain a frieze-pattern. Moreover, within the part of the frieze-pattern that is bounded by the line of slope -1 through u, the line of slope $+1$ through v, and the snake itself, each entry admits an enumerative interpretation relating to paths in the snake graph. Specifically, given any location w in the table in the aforementioned region, let u' be the leftmost place where the line through w of slope -1 meets the snake, and let v' be the leftmost place where the line through w of slope $+1$ meets the snake; then the entry at w is equal to the number of paths in the snake from u' to v'. For instance, in Figure 17 which shows what happens for the $LLLRR$ snake (with subscripts attached to some of the 1's for purposes of labeling), we find that 9 is the number of paths from 1_a to 1_c, 7 is the number of paths from 1_b to 1_c, 13 is the number of paths from 1_a to 1_d, and 10 is the number of paths from 1_b to 1_d. (The reader may find it instructive to compare this picture with the corresponding picture for the $RRRLL$ snake; the arithmetic calculations are different, but the number 13 still emerges as the rightmost entry.)

To see why this connection between dual snakes and frieze patterns holds, we can use Lindström's lemma [32] (rediscovered later by John and Sachs [28] and by Gessel and Viennot [22]). The $m = 2$ case of this lemma states that if we have a directed graph with sources s_1, s_2 and targets t_1, t_2, and there is no way to create a pair of vertex-disjoint paths that join s_1 to t_2 and s_2 to t_1 respectively, then the

number of ways to create a pair of vertex-disjoint paths that join s_1 to t_1 and s_2 to t_2 respectively is equal to the 2-by-2 determinant $p_{11}p_{22} - p_{12}p_{22}$, where p_{ij} denotes the number of paths from s_i to t_j. In our example, putting $s_1 = 1_a$, $s_2 = 1_b$, $t_1 = 1_d$, and $t_2 = 1_c$ [sic], we see that there is no way to create a path from 1_a to 1_c and a path from 1_b to 1_d that do not cross, so the hypotheses are satisfied. Furthermore, there is exactly 1 way to create a path from 1_a to 1_d and a path from 1_b to 1_c that do not cross, so we may conclude that $p_{11}p_{22} - p_{12}p_{22}$ equals 1, which (given that the p_{ij}'s are entries in our table) is exactly the frieze relation.

We mention two other combinatorial models of frieze patterns, for the sake of completeness: Gregory Price's paths model [10] and the model of Broline, Crowe and Isaacs [6]. The former (which has been significantly generalized by Schiffler and Thomas; see [37]) is related to the perfect matching model by the bijection of Carroll and Price, and the latter is closely related to the Conway-Coxeter marking scheme.

5. A Tropical Analogue

Since the sideways frieze relation involves only subtraction-free expressions in the cluster variables, our whole picture admits a tropical analogue (for background on tropical mathematics, see [36]) in which multiplication is replaced by addition, division by subtraction, addition by max, and 1 by 0. (One could use min instead of max, but max will be more useful for us.) In this new picture, the Ptolemy relation

$$d_{i,j}\, d_{k,l} + d_{j,k}\, d_{i,l} = d_{i,k}\, d_{j,l}$$

becomes the ultrametric relation

$$\max(d_{i,j} + d_{k,l}, d_{j,k} + d_{i,l}) = d_{i,k} + d_{j,l}.$$

Metrics satisfying this relation arise from finite collections of non-intersecting arcs that join points on the sides of the n-gon in pairs, where the endpoints of such an arc are not permitted to be vertices of the n-gon. We will call such a collection of arcs an *integral lamination*. Figure 18 shows an integral lamination of a hexagon.

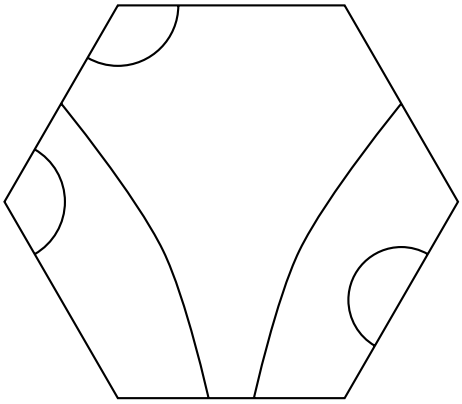

Figure 18. An integral lamination.

For any pair of vertices i, j, we define $d_{i,j}$ as the smallest possible number of intersections between a path in the n-gon from i to j and the arcs in the integral lamination (we choose the path so as to avoid crossing any arc in the integral lamination more than once). Then these quantities $d_{i,j}$ satisfy the ultrametric relation, and thus can be arranged to form a tropical frieze pattern satisfying the relation

$$\begin{array}{ccccc} X & & & & Y \\ & \ddots & A & \iddots & \\ & & B \quad C & & \\ & \iddots & D & \ddots & \\ Y & & & & X \end{array} \quad : \quad B + C = \max(A + D, X + Y)$$

For instance, the integral lamination of Figure 18 gives rise to the tropical frieze pattern

$$\begin{array}{ccccccccccccccccc} \ldots & & 3 & & 1 & & 1 & & 0 & & 2 & & 1 & & 3 & & \ldots \\ \ldots & & & 2 & & 2 & & 1 & & 2 & & 3 & & 2 & & & \ldots \\ \ldots & & 1 & & 3 & & 2 & & 1 & & 3 & & 2 & & 1 & & \ldots \\ \ldots & & & 2 & & 3 & & 2 & & 2 & & 2 & & 1 & & & \ldots \\ \ldots & & 0 & & 2 & & 1 & & 3 & & 1 & & 1 & & 0 & & \ldots \end{array}$$

As in the non-tropical case, we can find all the quantities $d_{i,j}$ once we know the values for all (i, j) associated with with the sides and diagonals belonging to some triangulation of the n-gon.

For an alternative picture, one can divide the laminated n-gon into a finite number of sub-regions, each of which is bounded by pieces of the boundary of the n-gon and/or arcs of the integral lamination; the vertices of the n-gon correspond to n special sub-regions (some of which may coincide with one another, if there is no arc in the integral lamination separating the associated vertices of the n-gon). Then the dual of this dissection of the n-gon is a tree with n specified leaf vertices (some of which may coincide), and $d_{i,j}$ is the graph-theoretic distance between leaf i and leaf j (which could be zero). We see that if we know $2n-3$ of these leaf-to-leaf distances, and the $2n-3$ pairs of leaves correspond to the sides and diagonals of a triangulated n-gon, then all of the other leaf-to-leaf distances can be expressed as piecewise-linear functions (involving just plus, minus, and max) of the $2n-3$ specified distances. (For more on the graph metric on trees, see [7].)

Going back to our lamination picture, we can associate to each arc a non-negative real numbers, called its weight. Such a weighted collection is a *measured lamination*. Then, for any pair of vertices i, j, we define $d_{i,j}$ as the sum of the weights of all the arcs that separate i from j. This again gives a metric that satisfies the ultrametric relation. In the dual (tree-metric) picture, this corresponds to assigning weights to edges, and measuring distance between leaves by summing weights along the path between them rather than merely counting the edges.

For an extensive generalization of the foregoing picture, see [18].

6. A Variant

An open problem concerns a variant of Conway and Coxeter's definition, in which the frieze recurrence is replaced by the recurrence

$$\begin{array}{ccccc} & & A & & \\ B & C & & D & : \quad E = (BD - C)/A \\ & & E & & \end{array}$$

and its sideways version

$$\begin{array}{ccccc} & & A & & \\ B & C & & D & : \quad D = (AE + C)/B \\ & & E & & \end{array} \quad .$$

We can construct arrays that have the same sort of symmetries as frieze patterns by starting with a suitable zig-zag of entries (where successive downwards steps can go left, right, or straight) and proceeding from left to right. For example, consider

the partial table

$$\begin{array}{cccccccc} ... & 1 & 1 & 1 & 1 & 1 & ... \\ & & A & D & x & & \\ & B & E & y & & & \\ & & C & F & z & & \\ ... & 1 & 1 & 1 & 1 & 1 & ... \end{array}$$

where $A, ..., F$ are pre-specified, and where we compute $y = (AC + E)/B$, $x = (y + D)/A$, $z = (y + F)/C$, etc. Then after exactly fourteen iterations of the procedure, one gets back the original numbers (in their original order). Moreover, along the way one sees Laurent polynomials with positive coefficients.

Define a "double zig-zag" to be a subset of the entries of an $(n-2)$-rowed table consisting of a pair of adjacent entries in each of the middle $n-4$ rows, such that the pair in each row is displaced with respect to the pair in the preceding and succeeding rows by at most one position. (Thus the entries A, B, C, D, E, F in the previous table form a double zig-zag, as do the entries D, E, F, x, y, z.)

Conjecture: Given any assignment of formal weights to the $2(n-4)$ entries in a double zig-zag in an $(n-2)$-rowed table, there is a unique assignment of rational functions to all the entries in the table so that the variant frieze relation is satisfied. These rational functions of the original $2(n-4)$ variables have glide-reflection symmetry that gives each row period $2n$. Furthermore, each of the rational functions in the table is a Laurent polynomial with positive coefficients.

There ought to be a way to prove this by constructing the numerators of these Laurent polynomials as sums of weights of perfect matchings of some suitable graph (or perhaps sums of weights of combinatorial objects more general than perfect matchings), and the numerators undoubtedly contain abundant clues as to how this can be done.

For $n = 5, 6, 7, 8$, it appears that the number of positive integer arrays satisfying the variant frieze relation is 1, 5, 51, 868 (respectively). This variant of the Catalan sequence does not appear to have been studied before. However, it should be said that these numbers were not computed in a rigorous fashion. Indeed, it is conceivable that beyond some point, the numbers becomes infinite (i.e., for some n there could be infinitely many $(n-2)$-rowed positive integer arrays satisfying the variant frieze relation).

Dean Hickerson [25] has shown that any $(n-2)$-rowed array that begins and ends with a row of 1's and satisfies the variant frieze relation in between has glide-reflection symmetry and period $2n$. This implies that if one generates such a variant frieze pattern starting with a double zig-zag of 1's, one gets a periodic array of positive rational numbers. However, it is not apparent that one can modify Hickerson's (purely algebraic) proof to show that these rational numbers are integers. Furthermore, if one uses formal weights instead of 1's, Hickerson's argument does not seem to show that the resulting rational functions are Laurent polynomials (let alone that

the Laurent polynomials have positive coefficients).

7. Markoff Numbers

A *Markoff triple* is a triple (x, y, z) of positive integers satisfying $x^2+y^2+z^2 = 3xyz$, such as the triple (2,5,29). A *Markoff number* is a positive integer that occurs in at least one such triple.

Writing the Markoff equation as $z^2-(3xy)z+(x^2+y^2) = 0$, a quadratic equation in z, we see that if (x, y, z) is a Markoff triple, then so is (x, y, z'), where $z' = 3xy - z = (x^2 + y^2)/z$, the other root of the quadratic in z. (z' is positive because $z' = (x^2 + y^2)/z$, and is an integer because $z' = 3xy - z$.) The same holds for x and y.

The following claim is well-known (for an elegant proof, see [1]): Every Markoff triple (x, y, z) can be obtained from the Markoff triple $(1, 1, 1)$ by a sequence of such exchange operations, in fact, by a sequence of exchange operations that leaves two numbers alone and increases the third. For example, $(1, 1, 1) \to (2, 1, 1) \to (2, 5, 1) \to (2, 5, 29)$.

Create a graph whose vertices are the Markoff triples and whose edges correspond to the exchange operations $(x, y, z) \leftrightarrow (x', y, z)$, $(x, y, z) \leftrightarrow (x, y', z)$, $(x, y, z) \leftrightarrow (x, y, z')$ where $x' = \frac{y^2+z^2}{x}$, $y' = \frac{x^2+z^2}{y}$, $z' = \frac{x^2+y^2}{z}$. This 3-regular graph is connected (see the claim in the preceding paragraph), and it is not hard to show that it is acyclic. Hence the graph is the 3-regular infinite tree.

This tree can be understood as the dual of the triangulation of the upper half plane by images of the modular domain under the action of the modular group. Concretely, we can describe this picture by using Conway's terminology of "lax vectors", "lax bases", and "lax superbases" ([11]).

A *primitive* vector $\mathbf{u}$ in a lattice L is one that cannot be written as $k\mathbf{v}$ for some vector $\mathbf{v}$ in L, with $k > 1$. A *lax vector* is a primitive vector defined only up to sign; if $\mathbf{u}$ is a primitive vector, the associated lax vector is written $\pm\mathbf{u}$. A *lax base* for L is a set of two lax vectors $\{\pm\mathbf{u}, \pm\mathbf{v}\}$ such that $\mathbf{u}$ and $\mathbf{v}$ form a basis for L. A *lax superbase* for L is a set of three lax vectors $\{\pm\mathbf{u}, \pm\mathbf{v}, \pm\mathbf{w}\}$ such that $\pm\mathbf{u}\pm\mathbf{v}\pm\mathbf{w} = \mathbf{0}$ (with appropriate choice of signs) and any two of $\mathbf{u}, \mathbf{v}, \mathbf{w}$ form a basis for L.

Each lax superbase $\{\pm\mathbf{u}, \pm\mathbf{v}, \pm\mathbf{w}\}$ contains the three lax bases $\{\pm\mathbf{u}, \pm\mathbf{v}\}$, $\{\pm\mathbf{u}, \pm\mathbf{w}\}$, $\{\pm\mathbf{v}, \pm\mathbf{w}\}$ and no others. In the other direction, each lax base $\{\pm\mathbf{u}, \pm\mathbf{v}\}$ is in the two lax superbases $\{\pm\mathbf{u}, \pm\mathbf{v}, \pm(\mathbf{u}+\mathbf{v})\}$, $\{\pm\mathbf{u}, \pm\mathbf{v}, \pm(\mathbf{u}-\mathbf{v})\}$ and no others.

The *topograph* is the graph whose vertices are lax superbases and whose edges are lax bases, where each lax superbase is incident with the three lax bases in it. This gives a 3-valent tree whose vertices correspond to the lax superbases of L, whose edges correspond to the lax bases of L, and whose "faces" correspond to the lax vectors in L.

The lattice L that we will want to use is the triangular lattice $L = \{(x, y, z) \in \mathbf{Z}^3 \ : \ x + y + z = 0\}$ (or $\mathbf{Z}^3/\mathbf{Z}\mathbf{v}$ where $\mathbf{v} = (1, 1, 1)$, if you prefer).

Using this terminology, it is now possible to state the main idea of this section (with details and proof to follow): Unordered Markoff triples are associated with lax superbases of the triangular lattice, and Markoff numbers are associated with lax vectors of the triangular lattice. For example, the unordered Markoff triple $2, 5, 29$ corresponds to the lax superbase $\{\pm\mathbf{u}, \pm\mathbf{v}, \pm\mathbf{w}\}$ where $\mathbf{u} = \vec{OA}$, $\mathbf{v} = \vec{OB}$, and $\mathbf{w} = \vec{OC}$, with O, A, B, and C forming a fundamental parallelogram for the triangular lattice, as shown in Figure 19. The Markoff numbers 1, 2, 5, and 29 correspond to the primitive vectors $\vec{AB}$, $\vec{OA} = \vec{BC}$, $\vec{OB} = \vec{AC}$, and $\vec{OC}$.

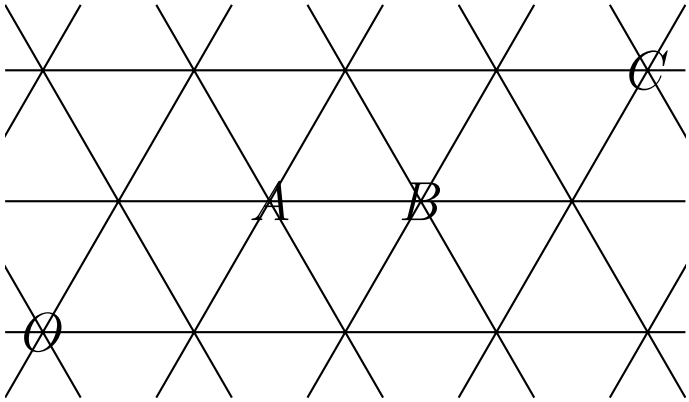

Figure 19. A fundamental parallelogram.

To find the Markoff number associated with a primitive vector $\vec{OX}$, take the union R of all the triangles that segment OX passes through. The underlying lattice provides a triangulation of R. For example, for the vector $\mathbf{u} = \vec{OC}$ from Figure 19, the triangulation is as shown in Figure 20.

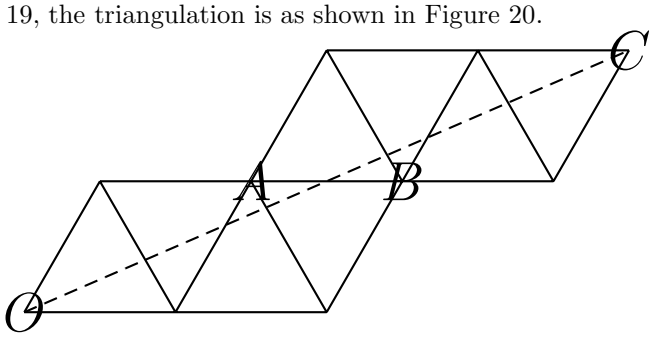

Figure 20. A Markoff snake.

Turn the triangulation into a planar bipartite graph as in Section 2, let $G(\mathbf{u})$ be the graph that results from deleting vertices O and C, and let $M(\mathbf{u})$ be the number of perfect matchings of $G(\mathbf{u})$. (If $\mathbf{u}$ is a shortest vector in the lattice, put $M(\mathbf{u}) = 1$.)

Theorem 4 (Carroll, Itsara, Le, Musiker, Price, and Viana [9] [10] [27] [33])**.** *If* $\{\mathbf{u}, \mathbf{v}, \mathbf{w}\}$ *is a lax superbase of the triangular lattice, then* $(M(\mathbf{u}), M(\mathbf{v}), M(\mathbf{w}))$ *is a Markoff triple. Every Markoff triple arises in this fashion. In particular, if* $\mathbf{u}$ *is a primitive vector, then* $M(\mathbf{u})$ *is a Markoff number, and every Markoff number arises in this fashion.*

(The association of Markoff numbers with the topograph is not new; what is new is the combinatorial interpretation of the association, by way of perfect matchings.)

Proof. The base case, with

$$(M(\mathbf{e}_1), M(\mathbf{e}_2), M(\mathbf{e}_3)) = (1, 1, 1),$$

is clear. The only non-trivial part of the proof is the verification that

$$M(\mathbf{u} + \mathbf{v}) = (M(\mathbf{u})^2 + M(\mathbf{v})^2)/M(\mathbf{u} - \mathbf{v}).$$

For example, in Figure 21, we need to verify that

$$M(\vec{OC})M(\vec{AB}) = M(\vec{OA})^2 + M(\vec{OB})^2.$$

But if we rewrite the desired equation as

$$M(\vec{OC})M(\vec{AB}) = M(\vec{OA})M(\vec{BC}) + M(\vec{OB})M(\vec{AC})$$

we see that this is just Kuo's lemma (see the proof of Theorem 1).

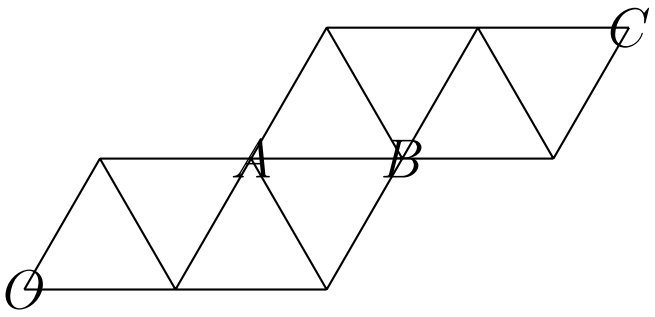

Figure 21. Kuo condensation for snakes.

□

Remark. Some of the work done by Carroll et al. during the years of the Research Experiences in Algebraic Combinatorics at Harvard (2001 to 2003) used the square lattice picture of Section 4; this way of interpreting the Markoff numbers combinatorially was actually conjectured first, in 2001–2002, by Musiker, and subsequently proved in 2002–2003 by Itsara, Le, Musiker, and Viana (see [33], [27], and [9], and Section 4 of this article). Subsequently, the group's first combinatorial model for frieze patterns, found by Price, involved paths rather than perfect matchings. It is reminiscent of, but apparently distinct from, the paths model considered in Section 4. Carroll turned Price's paths model into a perfect matchings model, which made it possible to arrive at the snake-graph model via a different route.

More generally, one can put $M(\mathbf{e}_1) = x$, $M(\mathbf{e}_2) = y$, and $M(\mathbf{e}_3) = z$ (with $x, y, z > 0$) and recursively define

$$M(\mathbf{u}+\mathbf{v}) = (M(\mathbf{u})^2 + M(\mathbf{v})^2)/M(\mathbf{u}-\mathbf{v}).$$

Then for all primitive vectors $\mathbf{u}$, $M(\mathbf{u})$ is a Laurent polynomial in x, y, z; that is, it can be written in the form $P(x, y, z)/\ x^a y^b z^c$, where $P(x, y, z)$ is an ordinary polynomial in x, y, z (with non-zero constant term). The numerator $P(x, y, z)$ of each Markoff polynomial is the sum of the weights of all the perfect matchings of the graph $G(\mathbf{u})$, where edges have weight x, y, or z according to orientation. The triples $X = M(\mathbf{u})$, $Y = M(\mathbf{v})$, $Z = M(\mathbf{w})$ of rational functions associated with lax superbases are solutions of the equation

$$X^2 + Y^2 + Z^2 = \frac{x^2+y^2+z^2}{xyz} XYZ.$$

Theorem 2 implies that these numerators $P(x, y, z)$ are polynomials with positive coefficients. This proves the following theorem:

Theorem 5. *Consider the initial triple (x, y, z), along with every triple of rational functions in x, y, and z that can be obtained from the initial triple by a sequence of operations of the form $(X, Y, Z) \mapsto (X', Y, Z)$, $(X, Y, Z) \mapsto (X, Y', Z)$, or $(X, Y, Z) \mapsto (X, Y, Z')$, where $X' = (Y^2 + Z^2)/X$, $Y' = (X^2 + Z^2)/Y$, and $Z' = (X^2 + Y^2)/Z$. Every rational function of x, y, and z that occurs in such a triple is a Laurent polynomial with positive coefficients.*

Fomin and Zelevinsky proved in [19] (Theorem 1.10) that the rational functions $X(x, y, z)$, $Y(x, y, z)$, $Z(x, y, z)$ are Laurent polynomials, but their methods did not prove positivity. An alternative proof of positivity, based on topological ideas, was given by Dylan Thurston [38].

It can be shown that if $\mathbf{u}$ is inside the cone generated by $+\mathbf{e}_1$ and $-\mathbf{e}_3$, then $a < b > c$ and $(c+1)\mathbf{e}_1 - (a+1)\mathbf{e}_3 = \mathbf{u}$. (Likewise for the other sectors of L.) This implies that all the "Markoff polynomials" $M(\mathbf{u})$ are distinct (aside from the fact that $M(\mathbf{u}) = M(-\mathbf{u})$), and thus $M(\mathbf{u})(x, y, z) \neq M(\mathbf{v})(x, y, z)$ for all primitive

vectors $\mathbf{u} \neq \pm\mathbf{v}$ as long as (x, y, z) lies in a dense G_δ set of real triples. This fact can be used to show [38] that, for a generic choice of hyperbolic structure on the once-punctured torus, no two simple geodesics have the same length. (It should be mentioned that for the specific choice $x = y = z = 1$, the distinctness of the numbers $M(\mathbf{u})(x, y, z)$ as $\mathbf{u}$ varies is the famous, and (as of 2005) still unproved, "unicity conjecture" for Markoff numbers.)

A slightly different point of view of Markoff numbers focuses on triangles rather than lax superbases: Say that points A, B, and C in the equilateral triangular lattice form a "fundamental triangle" if the area of triangle ABC equals the area of the equilateral triangles of which the lattice is composed. For example, the points A, B, and C in Figure 21 are the vertices of a fundamental triangle. (If four points form a fundamental parallelogram for the lattice, then any three of the four points form a fundamental triangle.) By Pick's theorem, a triangle is fundamental if and only if it has no lattice points in its interior and no lattice points on its boundary other than its three vertices. Let A, B, and C form a fundamental triangle. Define the "triangulation distance" $d(x, y)$ between two vertices x and y as $M(\mathbf{u})$ where $\mathbf{u}$ is the vector from x to y. Then the triangulation distances $d(A, B)$, $d(A, C)$, and $d(B, C)$ form a Markoff triple, and every Markoff triples arises in this way.

We conclude by mentioning a special sequence of Markoff numbers, obtained by following the tree along those branches that give greatest numerical increase: 1, 1, 2, 5, 29, 433, 37666, ... This sequence was considered by Dana Scott (see [21]), and satisfies the recurrence $f(n) = (f(n-1)^2 + f(n-2)^2)/f(n-3)$. Using the A and B matrices from Section 4, we see that we can alternately characterize the numbers as the upper-left entries in the sequence of matrices

$$\begin{pmatrix} 1 & 1 \\ 1 & 0 \end{pmatrix}, \begin{pmatrix} 1 & 0 \\ 0 & 1 \end{pmatrix}, \begin{pmatrix} 2 & 1 \\ 1 & 1 \end{pmatrix}, \begin{pmatrix} 5 & 2 \\ 2 & 1 \end{pmatrix}, \begin{pmatrix} 29 & 12 \\ 12 & 5 \end{pmatrix}, \begin{pmatrix} 433 & 179 \\ 179 & 74 \end{pmatrix}, \ldots$$

satisfying the multiplicative recurrence relation

$$M(n) = M(n-1)M(n-3)^{-1}M(n-1)$$

(note that the Fibonacci numbers satisfy the additive version of this recurrence). Andy Hone [26] has shown that $\log \frac{\log f(n)}{n}$ approaches $\log \frac{1+\sqrt{5}}{2}$ as $n \to \infty$.

8. Other Directions for Exploration

8.1. Non-integer Frieze-patterns

Given that the original geometric context of frieze patterns gives rise to arrays containing numbers that are not integers, it seems fairly natural to try to extend the Conway-Coxeter theory to this broader setting. Enumerative questions would

be a good place to start. One might for instance try to count all the frieze patterns of order n whose entries are either (positive) integers or half-integers, and see if the enumerating sequence is any sort of known analogue of the Catalan sequence. Also, since many geometric frieze patterns involve (irrational) algebraic numbers, it might also be natural to enumerate frieze patterns with entries in a given number ring (though this might not be so very natural after all: consider that, in its original geometric context, positivity of the entries of the frieze pattern is a consequence of their metric interpretation, whereas for algebraic number rings positivity is not a very robust notion since it depends on the embedding of the ring in $\mathbf{R}$).

8.2. Non-fundamental Triangles

Suppose A, B, and C are points in the lattice such that line segments AB, AB, and BC contain no lattice-points other than their endpoints, so that the triangulation distances $d(A,B)$, $d(A,C)$, $d(B,C)$ are well-defined. We have seen that if triangle ABC contains no lattice points in its interior, then these distances satisfy the Markoff equation. Can anything be said if this condition does not hold? For instance, in a lattice made of equilateral triangles of side-length 1, consider an equilateral triangle ABC of side-length $\sqrt{3}$ containing one interior point. The triangulation distances are all equal to 2, and $(2,2,2)$ is not a Markoff triple. Nevertheless, perhaps there is a different algebraic equation that this triple satisfies. More precisely, there may be an algebraic relation satisfied by the triangulation distances $x = d(B',C')$, $y = d(A',C')$, $z = d(A',B')$ where $A'B'C'$ is any image of ABC under the joint action of $SL_2(\mathbf{Z})$ (change of lattice-base) and $\mathbf{Z}^2$ (translation). Indeed, the whole numbers x, y, z satisfy the condition that there exist other whole numbers x', y', z' (namely, the triangulation distances from the interior point to A', B', and C' respectively) such that $x'^2 + y^2 + z^2 = 3x'yz$, $x^2 + y'^2 + z^2 = 3xy'z$, and $x^2 + y^2 + z'^2 = 3xyz'$, and perhaps some sort of quantifier elimination procedure would permit us to write this as a condition on just x, y, and z. More broadly, perhaps each orbit of triangles under the action of $SL_2(\mathbf{Z})$ and $\mathbf{Z}^2$ gives rise to triples satisfying a particular algebraic condition specific to that orbit.

8.3. Other Ternary Cubics

Neil Herriot showed [24] that if we replace the triangular lattice used above by the tiling of the plane by isosceles right triangles (generated from one such triangle by repeated reflection in the sides), fundamental triangles give rise to triples x, y, z of positive integers satisfying either

$$x^2 + y^2 + 2z^2 = 4xyz$$

or

$$2x^2 + 2y^2 + z^2 = 4xyz.$$

(Note that these two Diophantine equations are essentially equivalent, as the map $(x, y, z) \mapsto (x, y, 2z)$ gives a bijection between solutions to the former and solutions to the latter.) For instance, if for any two vertices X, Y we define the triangulation distance $d(X, Y)$ in analogy with the definition used before (now using the isosceles right triangle lattice in place of the equilateral triangle lattice), then the points O, A, B, C shown in Figure 22 satisfy $d(A, B) = 1$, $d(O, A) = 1$, $d(B, C) = 2$, $d(O, B) = 3$, $d(A, C) = 3$, and $d(O, C) = 11$, corresponding to the solution triples $(11)^2 + (3)^2 + 2(1)^2 = 4(11)(3)(1)$ and $2(11)^2 + 2(3)^2 + (2)^2 = 4(11)(3)(2)$.

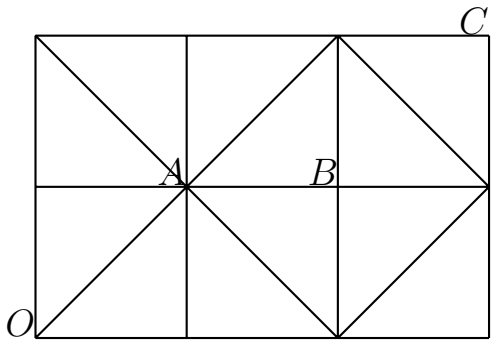

Figure 22. Herriot's theorem.

More specifically, Herriot showed that if ABC is a fundamental triangle, then the triangulation distances $d(A, B)$, $d(A, C)$, $d(B, C)$ satisfy

$$d(A, B)^2 + 2d(A, C)^2 + 2d(B, C)^2 = 4d(A, B)d(A, C)d(B, C)$$

or

$$2d(A, B)^2 + d(A, C)^2 + d(B, C)^2 = 4d(A, B)d(A, C)d(B, C)$$

according to whether the vertices A, B, C have respective degrees 4,4,8 or 8,8,4. (One can check that a fundamental triangle cannot have all three vertices of degree 4 or all three vertices of degree 8.) A related observation is that if $OACB$ is a fundamental parallelogram with O and A of degree 8 and B and C of degree 4, then $d(B, C) = 2d(O, A)$.

Herriot's result, considered in conjunction with the result on Markoff numbers, raises the question of whether there might be some more general combinatorial approach to ternary cubic equations of similar shape.

Rosenberger [34] showed that there are exactly three ternary cubic equations of the shape $ax^2 + by^2 + cz^2 = (a+b+c)xyz$ for which all the positive integer solutions

can be derived from the solution $(x, y, z) = (1, 1, 1)$ by means of the exchange operations $(x, y, z) \to (x', y, z)$, $(x, y, z) \to (x, y', z)$, and $(x, y, z) \to (x, y, z')$, with $x' = (by^2 + cz^2)/ax$, $y' = (ax^2 + cz^2)/by$, and $z' = (ax^2 + by^2)/cz$. These three ternary cubic equations are

$$x^2 + y^2 + z^2 = 3xyz,$$

$$x^2 + y^2 + 2z^2 = 4xyz,$$

and

$$x^2 + 2y^2 + 3z^2 = 6xyz.$$

Note that the triples of coefficients that occur here — (1,1,1), (1,1,2), and (1,2,3) — are precisely the triples that occur in the classification of finite reflection groups in the plane. Specifically, the ratios 1:1:1, 1:1:2, and 1:2:3 describe the angles of the three triangles — the 60-60-60 triangle, the 45-45-90 triangle, and the 30-60-90 triangle — that arise as the fundamental domains of the three irreducible two-dimensional reflection groups.

Since the solutions to the ternary cubic $x^2+y^2+z^2 = 3xyz$ describe properties of the tiling of the plane by 60-60-60 triangles, and solutions to the ternary cubic $x^2 + y^2 + 2z^2 = 4xyz$ describe properties of the tiling of the plane by 45-45-90 triangles, the solutions to the ternary cubic $x^2 + 2y^2 + 3z^2 = 6xyz$ "ought" to be associated with some combinatorial model involving the reflection-tiling of the plane by 30-60-90 triangles. Unfortunately, the most obvious approach (based on analogy with the 60-60-60 and 45-45-90 cases) does not work. So we are left with two problems that may or may not be related: first, to find a combinatorial interpretation for the integers (or, more generally, the Laurent polynomials) that arise from solving the ternary cubic $x^2 + 2y^2 + 3z^2 = 6xyz$; and second, to find algebraic recurrences that govern the integers (or, more generally, the Laurent polynomials) that arise from counting (or summing the weights of) perfect matchings of graphs derived from the reflection-tiling of the plane by 30-60-90 triangles.

If there is a way to make the analogy work, one might seek to extend the analysis to other ternary cubics. It is clear how this might generalize on the algebraic side. On the geometric side, one might drop the requirement that the triangle tile the plane by reflection, and insist only that each angle be a rational multiple of 360 degrees. There is a relatively well-developed theory of "billiards flow" in such a triangle (see e.g. [29]) where a particle inside the triangle bounces off the sides following the law of reflection (angle of incidence equals angle of reflection) and travels along a straight line in between bounces. The path of such a particle can be unfolded by repeatedly reflecting the triangular domain in the side that the particle is bouncing off of, so that the unfolded path of the particle is just a straight line in the plane. Of special interest in the theory of billiards are trajectories joining a corner to a corner (possibly the same corner or possibly a different one); these

are called saddle connections. The reflected images of the triangular domain form a triangulated polygon, and the saddle connection is a combinatorial diagonal of this polygon. It is unclear whether the combinatorics of such triangulations might contain dynamical information about the billiards flow, but if this prospect were to be explored, enumeration of matchings on the derived bipartite graphs would be one thing to try.

8.4. More Variables

Another natural variant of the Markoff equation $x^2+y^2+z^2 = 3xyz$ is the equation $w^2 + x^2 + y^2 + z^2 = 4wxyz$ (one special representative of a broader class called Markoff-Hurwitz equations; see [1]). The Laurent phenomenon applies here too: the four natural exchange operations convert an initial formal solution (w, x, y, z) into a quadruple of Laurent polynomials. (This is a special case of Theorem 1.10 in [19].)

Furthermore, the coefficients of these Laurent polynomials appear to be positive, although as of 2005 this has not been proved.

The numerators of these Laurent polynomials ought to be weight-enumerators for some combinatorial model, but it is unclear how to reverse-engineer the combinatorial model from the Laurent polynomials.

References

[1] A. Baragar, Integral solutions of the Markoff-Hurwitz equations, *J. Number Theory* **49** (1994), 27–44.

[2] K. Baur and R.J. Marsh, Ptolemy relations for punctured discs, arXiv:0711.1443.

[3] A. Benjamin and J. Quinn, Proofs That Really Count. Mathematical Association of America, Washington, D.C., 2003.

[4] A. Benjamin, J. Quinn, and F. Su, Counting On continued fractions, *Math. Mag.* **73** (2000), 98–104.

[5] A. Benjamin and D. Zeilberger, Pythagorean primes and palindromic continued fractions, *Integers* **5** (2005), A30.

[6] D. Broline, D.W. Crowe, and I.M. Isaacs, The geometry of frieze patterns, *Geom. Dedicata* **3** (1974), 171–176.

[7] P. Buneman, A note on metric properties of trees, *J. Combin. Theory Ser. B* **17** (1974), 48–50.

[8] P. Caldero and F. Chapoton, Cluster algebras as Hall algebras of quiver representations, arXiv:math.RT/0410187.

[9] G. Carroll, A. Itsara, I. Le, J. Propp, Markov numbers, Farey sequences, and the Ptolemy recurrence, unpublished memo (2003).

[10] G. Carroll and G. Price, Two new combinatorial models for the Ptolemy recurrence, unpublished memo (2003).

[11] J. Conway, The Sensual (Quadratic) Form, Mathematical Association of America, Washington, D.C., 1997.

[12] J.H. Conway and H.S.M. Coxeter, Triangulated polygons and frieze patterns, *Math. Gaz.* **57** (1973), 87–94.

[13] J.H. Conway and R.K. Guy, The Book of Numbers, Springer-Verlag, New York, 1996.

[14] H.S.M. Coxeter, Regular Polytopes, Macmillan, New York, 1963; reprinted by Dover.

[15] H.S.M. Coxeter, Frieze patterns, *Acta Arith.* **18** (1971), 297–310.

[16] H.S.M. Coxeter, Cyclic sequences and frieze patterns, *Vinculum* **8** (1971), 4–7.

[17] H.S.M. Coxeter, Regular Complex Polytopes, Cambridge University Press, London, 1974.

[18] S. Fomin, M. Shapiro, and D. Thurston, Cluster algebras and triangulated surfaces, Part I: Cluster complexes, arXiv:`math/0608367`.

[19] S. Fomin and A. Zelevinsky, The Laurent phenomenon, arXiv:`math.CO/0104241`.

[20] S. Fomin and A. Zelevinsky, Y-systems and generalized associahedra, arXiv:`hep-th/0111053`.

[21] D. Gale, The strange and surprising saga of the Somos sequences, *Math. Intell.* **13**, 40–42 (1991), and Somos sequence spdate, *Math. Intell.* **13,** 49–50 (1991)). Republished (see pages 2–5, 22–24) in D. Gale, Tracking the Automatic Ant. Springer-Verlag, 1998.

[22] I.M. Gessel and X. Viennot, Binomial determinants, paths, and hook length formulae, *Adv. Math.* **58** (1985), 300–321.

[23] M. Gordon and W.H.T. Davison, Theory of resonance topology of fully aromatic hydrocarbons, *J. Chem. Phys.* **20** (1952), 428–435.

[24] N. Herriot, personal communication; preliminary write-up at `http://jamespropp.org/reach/Herriot/ptolemywriteup.html`.

[25] D. Hickerson, personal communication.

[26] A. Hone, Diophantine nonintegrability of a third order recurrence with the Laurent property, *J. Phys. A* **39** (2006), L171–L177. `arXiv:math.NT/0601324`.

[27] A. Itsara, G. Musiker, J. Propp, and R. Viana, Combinatorial interpretations for the Markoff numbers, memo dated May 1, 2003; `http://jamespropp.org/reach/Itsara/markovversion3.pdf`.

[28] P. John and H. Sachs, Wegesysteme und Linearfaktoren in hexagonalen und quadratischen Systemen (Path systems and linear factors in hexagonal and square systems), in: Graphen in Forschung und Unterricht (Festschrift K. Wagner), Barbara Franzbecker Verlag Bad Salzdetfurth 1985; pp. 85–101.

[29] R. Kenyon and J. Smillie, Billiards on rational-angled triangles, *Comment. Math. Helv.* **75** (2000), 65–108.

[30] E. Kuo, Applications of graphical condensation for enumerating matchings and tilings, *Theoret. Comput. Sci.* **319** (2004), 29–57; arXiv:`math.CO/0304090`.

[31] G. Kuperberg, Kasteleyn cokernels, *Electron. J. Combin.* **9** (2002), article R29; arXiv:math.CO/0108150.

[32] B. Lindström, On vector representations of induced matroids, *Bull. Lond. Math. Soc.* **5** (1973) 85–90.

[33] G. Musiker, A conjectured combinatorial interpretation for Markov numbers, memo dated June 27, 2002; http://jamespropp.org/reach/Musiker/NewResults.pdf.

[34] G. Rosenberger, Uber die diophantische Gleichung $ax^2 + by^2 + cz^2 = dxyz$, *J. Reine Angew. Math.* **305** (1979), 122–125.

[35] H. Sachs, Perfect matchings in hexagonal systems, *Combinatorica* **4** (1984), 89–99.

[36] D. Speyer and B. Sturmfels, Tropical mathematics, arXiv:math.CO/0408099.

[37] R. Schiffler and H. Thomas, On cluster algebras arising from unpunctured surfaces, arXiv:0712.4131.

[38] D. Thurston, personal communication.

[39] K. Wagner, Bemerkungen zum Vierfarbenproblem, *Jahresber. Dtsch. Math.-Ver.* **46** (1936), 26–32.

[40] D. Zeilberger, A combinatorial approach to matrix algebra, *Discrete Math.* **56** (1985), 61–72.

[41] D. Zeilberger, Dodgson's determinant-evaluation rule proved by two-timing men and women, *Electron. J. Combin.* **4**:2 (1997), R22; arXiv:math.CO/9808079.